Department of Oncology, Jinshan Hospital Affiliated to Fudan University, Shanghai City, P.R. China

Effects and mechanism of ensartinib (X-396) on the adhesion and metastasis of non-small cell lung cancer cells

Bin Zhang*, Tiankui Qiao, Caixia Gao

Received March 22, 2019, accepted April 26, 2019

**Corresponding author: Dr. Bin Zhang, Department of Oncology, Jinshan Hospital Affiliated to Fudan University, no. 1508 Longhang Road, Jinshan District, Shanghai City, 201508, P.R. China*
ag20181230@sina.com

Pharmazie 74: 543-546 (2019) *doi: 10.1691/ph.2019.9461*

The current study aimed to investigate the inhibitory effect and mechanism of ensartinib on adhesion, invasion and migration of non-small cell lung cancer (NSCLC) cells, including H460 and A549. Cell adhesion test, scratch test and Transwell cell invasion test were used to detect cell adhesion, migration and invasion. RT-PCR was used to detect the expression of MMP-2 and MMP-9 in H460 and A549 cells. Western blot was used to detect the expression of MMP-2 and MMP-9 proteins, ERK signaling pathway related proteins and p-Akt. Our data showed that ensartinib inhibited adhesion, invasion and migration of H460 and A549 cells in a concentration-dependent manner ($P < 0.05$). Ensartinib decreased the expression of MMP-2 and MMP-9 in H460 and A549 cells ($P < 0.01$). It also downregulated the expression of MMP-2 and MMP-9 in H460 and A549 cells, and inhibited the expression of Ras, p-c-Raf, p-ERK 1/2 and p-Akt upstream in a concentration- and time-dependent manner. Ensartinib inhibits the adhesion, invasion and migration of NSCLC cells, and such effect is related to downregulation of MMP-2 and MMP-9 expression, inhibition of ERK signaling pathway and p-Akt expression.

1. Introduction

Lung cancer is one of the most morbidity and mortality malignant tumors in the world (Wang et al. 2016). Every year more than one million people die of lung cancer (Alibolandi et al. 2015). Among them, non-small cell lung cancer (NSCLC) accounts for 80 to 85% of lung cancer, and its 5-year survival rate is less than 15 % (He et al. 2018). About 30 % of patients with NSCLC had distant metastasis at the time of diagnosis, 50 to 60% of patients had distant metastasis during treatment, and eventually 80 to 90% of patients die of lung cancer metastasis (Howe et al. 2016). Therefore, inhibiting and preventing the metastasis of lung cancer cells is the key to treat NSCLC and improve the survival rate of patients.

Tumor metastasis is regulated by many factors and steps, including the decrease of adhesion between tumor cells, the enhancement of adhesion with extracellular matrix (ECM), the degradation of ECM and basement membrane, the enhancement of migration and invasion ability of tumor cells (Hsu et al. 2007; Dowlati et al. 2008). Therefore, inhibiting NSCLC cell adhesion, invasion and migration is the basis of suppressing lung cancer metastasis (Jassam et al. 2017; He et al. 2018).

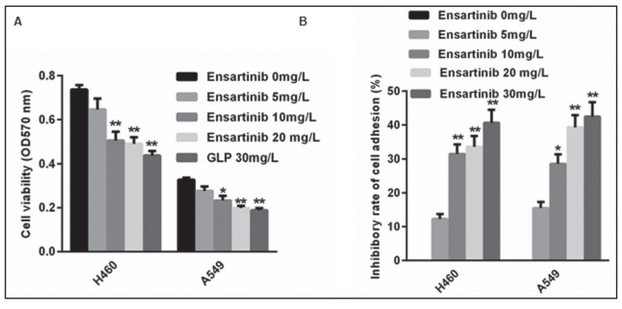

Fig. 1: Effect of ensartinib on adhesion of H460 and A549 cells. (A) Cell viability was determined using MTT assay. (B) The inhibition rate of cell adhesion increased gradually with the treatment of different ensartinib concentrations (0, 5, 10, 20, 30 mg/L). *p<0.05, **p<0.01 vs. Ensartinib 5 mg/L.

Although the first generation ALK tyrosine kinase inhibitor clozotinib has a good effect in the early stage of treatment among NSCLC patients, most patients will acquire drug resistance after continuous treatment (Singhi and Horn 2018). Recently, ensartinib, a new drug that has entered the phase III phase of clinical trials, may be expected to surpass clozotinib and become a new therapy option for ALK-positive NSCLC patients (Horn et al. 2018). However, the specific underlying mechanism of ensartinib on NSCLC progression remains largely unknown.

2. Investigations and results

2.1. Effect of ensartinib on adhesion of H460 and A549 cells

Different concentrations of ensartinib (0, 5, 10, 20, 30 mg/L) were used to treat H460 and A549 cells for 24 h. Cell adhesion was then examined. The results showed that after ensartinib treatment, the adhesion ability of H460 and A549 cells decreased gradually, that is, the inhibition rate of cell adhesion increased gradually and concentration dependently (Fig. 1). There was a significant difference among the groups ($P < 0.05$).

2.2. Effect of ensartinib on migration ability of H460 and A549 cells

The effect of ensartinib on the migration ability of H460 and A549 cells was examined by scratch test. As shown in Fig. 2, after ensartinib (30 mg/L) treatment for 0, 6, 12, 24 and 48 h, the scratch width gradually increased and the cell density on both sides of the scratch decreased (Fig. 2A). On the contrary, the scratch width gradually decreased and the cell density on both sides of the scratch increased after 0, 6, 12, 24 and 48 h in the control group of H460 and A549 cells (Fig. 2A). At the same time, the healing rate of scratches increased gradually in the control group of H460 and A549 cells, and decreased gradually in the ensartinib (30 mg/L) group (Fig 2B).

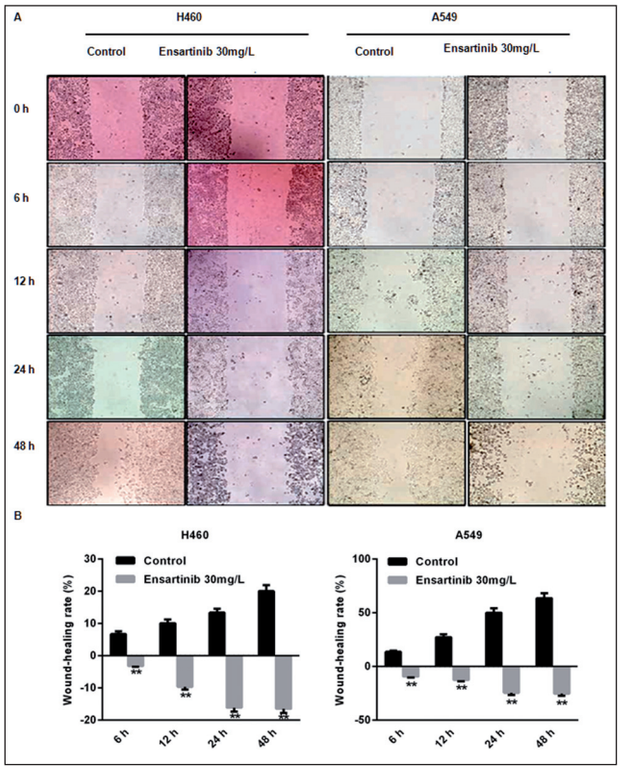

Fig. 2: Effect of ensartinib on migration ability of H460 and A549 cells. (A) Scratch test was performed to evaluate the effects of ensartinib (30 mg/L) treatment for 0, 6, 12, 24 and 48 h in H460 and A549 cells. (B) Wound-healing rate was calculated. **p<0.01 vs. control.

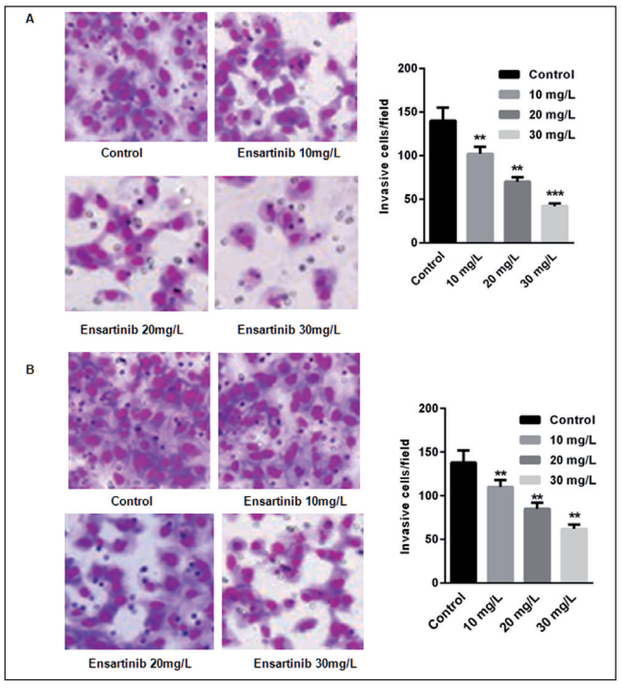

Fig. 3: Effect of ensartinib on invasive ability of H460 and A549 cells. Transwell cell invasion assay was used to detect the changes of ensartinib's invasive ability to H460 (A) and A549 (B) cells. **p<0.01 vs. control.

2.3. Effect of ensartinib on invasive ability of H460 and A549 cells

Transwell cell invasion assay was used to detect the changes of ensartinib's invasive ability to H460 and A549 cells. The results showed that after 24 h of ensartinib (0, 10, 20, 30 mg/L), the number of cells passing through the membrane in the treatment group of H460 and A549 cells was significantly lower than that in the control group ($P < 0.01$), and showed a concentration-dependent (Fig. 3A and 2B).

2.4. Regulation of ensartinib on MMP-2 and MMP-9 mRNA levels in H460 and A549 cells

RT-PCR was used to further study the regulation of ensartinib on the levels of metalloproteinase-2 (MMP-2) and metalloproteinase-9 (MMP-9) in H460 and A549 cells, which are closely related to the adhesion, invasion and migration of cancer cells. As shown in Figs 4A and 4B, ensartinib effectively inhibited the mRNA levels of MMP-9 and MMP-2 in H460 and A549 cells with the increase of ensartinib concentration (20, 30 mg/L) compared with that of control.

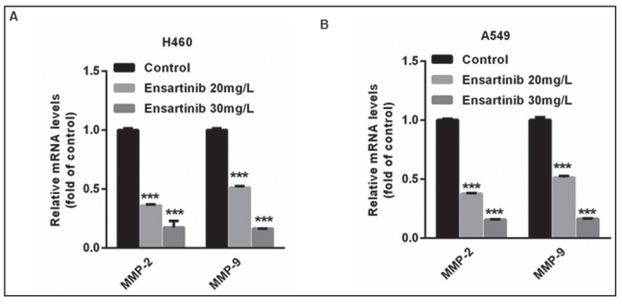

Fig. 4: Regulation of ensartinib on MMP-2 and MMP-9 mRNA levels in H460 and A549 cells. Real time PCR analysis demonstrated that ensartinib effectively inhibited the mRNA levels of MMP-9 and MMP-2 in H460 (A) and A549 (B) cells with the increase of ensartinib concentration (20, 30 mg/L) compared with that of control. **p<0.01 vs. control.

2.5. Ensartinib regulates the expression of MMP-2 and MMP-9 and ERK signaling pathway-related proteins and p-Akt in H460 and A549 cells

To further explore the mechanism of ensartinib inhibiting adhesion, migration and invasion of H460 and A549 cells, the expression of MMP-2 and MMP-9 was detected by Western blot. The results showed that ensartinib downregulated the expression of MMP-2 and MMP-9 in a time-dependent manner (Figs. 5A and 5B). At the same time, we further explored the changes of Ras and p-ERK 1/2 and p-Akt expression in upstream ERK signaling pathway after ensartinib inhibited MMP-2 and MMP-9 proteins. As shown in Figs. 5A and 5B, the expression levels of Ras, p-c-Raf, p-ERK 1/2 and p-Akt decreased in H460 and A549 cells treated with ensartinib, indicating that ensartinib inhibited the expression of ERK signaling pathway and p-Akt in a time-dependent manner.

3. Discussion

NSCLC accounts for 80 to 85 % of lung cancer, which has the characteristics of low survival rate and high metastasis rate (Kuang et al. 2013). Ensartinib is a newly developed lung cancer drug, which can effectively inhibit 17 ALK fusion types with IC50 < 4 nM (Singhi and Horn 2018). There is not much information about this drug. Recently, phase I/II clinical trials in humans have just been published (Horn et al. 2018). Patients without ALK targeted therapy can achieve 80 % efficiency and show good brain metastasis control ability (Horn et al. 2018). However, the specific effects and underlying mechanism of ensartinib on NSCLC deserve further study.

Tumor metastasis is a multi-gene, multi-factor, multi-step biological process. Reducing the adhesion between cancer cells and extracellular matrix (ECM) is the beginning of cancer metastasis (Lin et al. 2017). In this study, cell adhesion experiments were conducted to investigate the changes of adhesion in H460 and A549 cells after ensartinib treatment. The results showed that

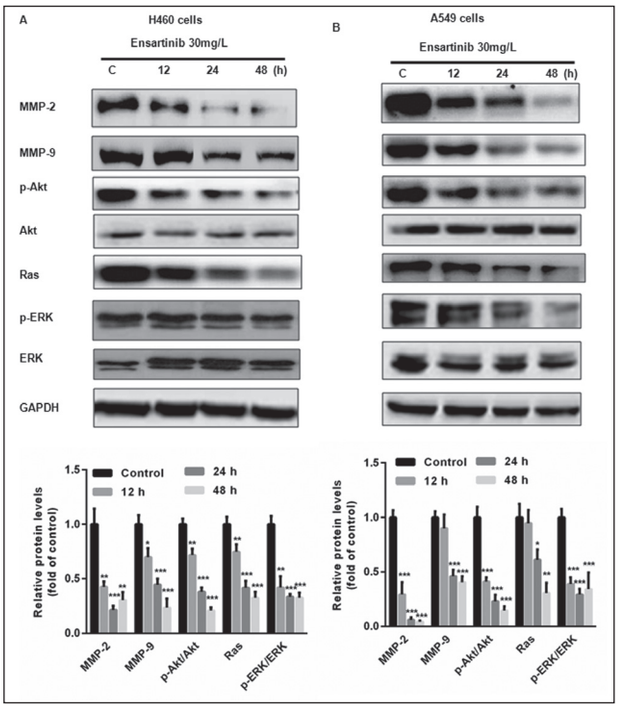

Fig. 5: Ensartinib regulates the expression of MMP-2 and MMP-9 and ERK signaling pathway-related proteins and p-Akt in H460 and A549 cells. The expression levels of MMP-2, MMP-9, Ras, p-c-Raf, p-ERK 1/2 and p-Akt decreased in H460 and A549 cells treated with ensartinib. *P<0.05, **p<0.01, ***P<0.001 vs. control.

ensartinib reduced the adhesion of both cells in a concentration-dependent manner. When cancer cells adhere to ECM, they invade ECM and basement membrane, secrete a variety of proteolytic enzymes, degrade ECM and basement membrane, and make cells break through the damaged basement membrane to detach and migrate from the primary lesion, and then metastasize with blood or lymphatic circulation (Min et al. 2018). Therefore, reducing the invasive and migratory ability of cancer cells is the key to inhibit cancer metastasis (Zhang et al. 2016). In this study, scratch test and Transwell cell invasion test showed that ensartinib effectively inhibited the migration and invasion of H460 and A549 cells.

The changes of ECM and basement membrane play an important role in the invasion and metastasis of tumors. Type IV collagen fibers are among the important components of ECM and basement membrane, and MMP-2/MMP-9 in matrix metalloproteinases (MMPs) can degrade them effectively (Wang et al. 2016; Zhou et al. 2018). Studies have confirmed that MMP-2 and MMP-9 not only degrade ECM and basement membrane, participate in tumor adhesion, invasion and vascular invasion, but are also related to the growth of primary and metastatic tumors, angiogenesis and malignant transformation of tumors (Ishiguro et al. 2013; Howe et al. 2016; Chae et al. 2018). In addition, increased expression of MMP-2 and MMP-9 was found in many invasive and highly metastatic tumors (Su et al. 2014; Ntantie et al. 2018). Meanwhile, the expression levels of MMP-2 and MMP-9 are closely related to the staging, metastasis and prognosis of lung cancer. Therefore, inhibiting the expression of MMP-2 and MMP-9 is the key to inhibit the invasion and migration of NSCLC (Tachezy et al. 2014; Webber et al. 2015). RT-PCR and Western blot showed that ensartinib not only reduced the expression of MMP-9 and MMP-2 in H460 and A549 cells at the mRNA level, but also downregulated the expression of MMP-2 and MMP-9 in H460 and A549 cells at the protein level in a time- and concentration-dependent manner. Therefore, ensartinib inhibits the adhesion, invasion and migration of NSCLC cells by suppressing the expression of MMP-2 and MMP-9.

Many studies have shown that the expression of MMP-9 and MMP-2 is mainly regulated by the upstream serine/threonine protein kinase family (MAPKs) signaling pathway (Fang et al. 2017; Ruder et al. 2018). Activation of the MAPKs pathway can upregulate the expression of MMP-2 and MMP-9, promote the invasion and migration of cancer cells (Zhang et al. 2010). On the contrary, inactivation of the MAPKs pathway inhibits the invasion and metastasis of cancer (Zheng et al. 2017). MAPKs signaling pathways mainly include extracellular signal-regulated kinase (ERK) pathway, p38 MAPK pathway and c-Jun-N terminal kinase (JNK) pathway (Zheng et al. 2017). Moreover, ERK signaling pathway, Ras/Raf/ERK signaling pathway, play a major role in the proliferation, differentiation, invasion, migration and apoptosis of many tumors (Zheng et al. 2017). Further studies on Ras/Raf/ERK signaling pathway showed that ensartinib could downregulate the expression of Ras, p-c-Raf and p-ERK 1/2 in H460 and A549 cells in a concentration- and time-dependent manner. Therefore, the inhibition of MMP-9 and MMP-2 expression by ensartinib may be related to the inhibition of upstream ERK signaling pathway.

In addition, Akt is suggested to promote invasion and migration of tumors by activating MMP-9 and MMP-2 (Cho et al. 2009; Kitano et al. 2014). Therefore, inhibiting the expression of Akt is regarded as a regulatory target to inhibit the metastasis of tumors (Cho et al. 2009; Kitano et al. 2014). It is also found that the activation of Akt, i.e. phosphorylated Akt (p-Akt), is closely related to the metastasis of NSCLC. Overexpression of p-Akt can improve the adhesion, invasion and metastasis of NSCLC (Kitano et al. 2014). This study showed that ensartinib inhibited the activation of p-Akt in H460 and A549 cells in a concentration- and time-dependent manner.

In conclusion, the results of this study demonstrate for the first time that ensartinib inhibits the adhesion, invasion and migration of NSCLC cells H460 and A549 by downregulating the expression of MMP-2 and MMP-9 genes and proteins and inhibiting the upstream ERK signaling pathway and p-Akt expression. These results indicate that ensartinib has a good anti-NSCLC adhesion and metastasis effect, which provides experimental basis and basis for further drug development and clinical application of ensartinib.

4. Experimental

4.1. Cell culture

Lung adenocarcinoma A549 cells and lung large cell lung cancer H460 cells were purchased from the Institute of Biochemistry and Cell Biology and Shanghai Academy of Life Sciences, Chinese Academy of Sciences, respectively. A549 cells were cultured in RPMI 1640 medium containing 10 % fetal bovine serum. Cells grew adherently in an incubator at 37 °C and 5 % CO_2 humidity. When cells reached 80 % confluence, they were digested with trypsin containing 0.125% EDTA and passaged in a dilution ratio of 1:4.

4.2. Ensartinib

Ensartinib (M1743, AbMole, http://abmole.bioon.com.cn/) was dissolved in DMSO and diluted to the corresponding concentration.

4.3. Cell adhesion test

A 96-well culture plate was coated with 50 µL collagen I solution in each hole, incubated in incubator at 37 °C and 5 % CO_2 for 1 h and washed with PBS twice. After that, 0.2 mL 3 % BSA was added and incubated for 2 h, and then washed with PBS twice for reserve. The H460 and A549 cells treated with different concentrations of ensartinib (0, 5, 10, 20, 30 mg/L) for 24 h were diluted with DMEM solution containing 10 % fetal bovine serum. The cell concentration was adjusted to 8 *10^8/L. The cells were added to 96-well coated plates with 100 µL per well. Each group was fed with 5 parallel pores, incubated at 37 °C and 5 % CO_2 for 2 h. After incubation, the culture medium was discarded and washed with PBS, with the non-adherent cells removed. Then, 50 µL MTT was added to each well and incubated in cell incubator for 3 h. After dissolving and crystallizing, the OD value of each well at 570 nm was measured. With ensartinib (0 mg/L) group as blank control group, the inhibition rate of adhesion was equal to (1 – OD value of experimental group / OD value of control group) *100 %.

4.4. Scratch test

The H460 and A549 cells in logarithmic growth phase were inoculated into 6-well plates at a density of 1 x 10^6 cells per well. When the cell adherence reached 90% confluence, the 20µL pipette was used to draw a vertical line in the middle of each well. Then, the cells were washed with PBS three times and the fallen cells were removed. Then, ensartinib (0, 30 mg/L) was added and incubated in 37 °C, 5 % CO_2 incubator for further culture. Scratch widths were observed and photographed (x 100) at 0, 6, 12, 24 and 48 h after ensartinib treatment. The experiment was repeated three

times in each group. The average widths of three parallel scratches were calculated respectively (three fixed positions were taken for each scratch to calculate the widths). Scratch healing rate / % = (initial scratch width – Scratch width at specified time) / initial scratch width * 100 %.

4.5. Transwell assay

The cell suspension was treated with ensartinib (0, 5, 10, 20, 30 mg/L) in the upper chamber. The cell suspension was incubated for 72 h at 37 °C and 5 % CO_2. The filter membrane was taken out, fixed with methanol and stained with Giemsa. Under micromicroscopy, each filter membrane was randomly divided into five fields (x 200), and the number of cells penetrating the membrane was counted. The average number was taken to indicate the invasive ability of each tumor cell.

4.6. RT-PCR

RNA was extracted by RNAVzol. The absorbance ratio of RNA at 260 and 280 nm was measured, and its purity and concentration were determined. The primer sequences were listed as follows: Human-GAPDH primer, sense primer: 5′-ATCGTGGAAGGACTCA-3′, antisense primer: 5′-CCAGTAGAGGCAGGGATGAT-3′; human-MMP2 primer sense primer:5′-CTACTGAGTGGCCGTGTTTG-3′, antisense primer: 5′-GGAAGCTCTGACCTTTCCAG-3′; human-MMP9 primer, sense primer: 5′-TCTTCCAAGGCCAATCCTAC-3′, antisense primer: 5′-ATCACCGTCGAGTCAGCTC-3′, cDNA synthesis conditions were listed as follows: RNA was reversed-transcribed into cDNA using the TaqMan RNA Reverse Transcription kit (Applied Biosystems; Thermo Fisher Scientific, Inc.). qPCR was performed using SYBR Green Supermix (Bio-Rad Laboratories, Inc., Hercules, CA, USA) and the iCycleriQ Real-Time PCR system (Bio-Rad Laboratories, Inc.) as described previously (Guo, Li et al. 2014). The detailed PCR procedures were at 95 ˚C for 10 min followed by 50 cycles of 95 ˚C for 10 s, 55 ˚C for 10 s, 72 ˚C for 5 s; 99 ˚C for 1 s; 59 ˚C for 15 s; 95 ˚C for 1 s; then cooling to 40 ˚C. Relative mRNA expression was normalized against the endogenous control, GAPDH, using the $2^{-\Delta\Delta Ct}$ method (Livak and Schmittgen 2001).

4.7. Western blot

Cells in the logarithmic growth phase were digested and inoculated into 6-well plate. Cell density was 5 x 10^8 /L. After a certain period of treatment, PBS was collected and washed twice. Cell lysate was added to each well and centrifuged for 20 min at 12,000 x g. Quantitative analysis of protein: Protein samples were taken and added into 4 x buffer solution, denatured at 100 °C for 5 min. Then, the protein samples were isolated on 15 % polyacrylamide SDS gel electrophoresis and transferred to the PVDF membrane. The membranes were blocked with 8 % skimmed milk in Tris-buffered saline with Tween-20 (TBST; pH 7.5) for 2 h at room temperature and were incubated with the following primary antibodies. Following several washes with TBST, the membranes were incubated with horserasish-peroxidase (HRP)-conjugated goat anti-rabbit and anti-mouse IgG or HRP-conjugated mouse anti-goat IgG (all 1:5,000; Origene Technologies, Inc.) for 2 h at room temperature and then washed. Protein bands were visualized using enhanced chemiluminscence (EMD Millipore, Billerica, MA, USA) according to the manufacturer's protocol. GAPDH was used as an internal control.

4.8. Statistical analysis

Data were analyzed using SPSS software (version 13.0; SPSS, Inc., Chicago, IL, USA). Data are expressed as the mean±standard error of the mean. The two-tailed unpaired student's t-tests were used for comparisons of two groups. The one way ANOVA multiple comparison test (SPSS 13.0) followed by Turkey post hoc test were used for comparisons of two more groups. $p<0.05$ was considered significant.

Conflicts of interest: None declared

References

Alibolandi M, Ramezani M, Abnous K, Sadeghi F, Atyabi F, Asouri M, Ahmadi AA, Hadizadeh F (2015) In vitro and in vivo evaluation of therapy targeting epithelial-cell adhesion-molecule aptamers for non-small cell lung cancer. J Control Release 209: 88-100.

Chae YK, Choi WM, Bae WH, Anker J, Davis AA, Agte S, Iams WT, Cruz M, Matsangou M, Giles FJ (2018) Overexpression of adhesion molecules and barrier molecules is associated with differential infiltration of immune cells in non-small cell lung cancer. Sci Rep 8: 1023.

Cho Y, Park MJ, Park M, Min SS, Yee J, Kim C, Han MS, Han SH (2009) Effects of CAY10404 on the PKB/Akt and MAPK pathway and apoptosis in non-small cell lung cancer cells. Respirology 14: 850-858.

Dowlati A, Gray R, Sandler AB, Schiller JH, Johnson DH (2008) Cell adhesion molecules, vascular endothelial growth factor, and basic fibroblast growth factor in patients with non-small cell lung cancer treated with chemotherapy with or without bevacizumab--an Eastern Cooperative Oncology Group Study. Clin Cancer Res 14: 1407-1412.

Fang Y, Wang J, Wang G, Zhou C, Wang P, Zhao S, Zhao S, Huang S, Su W, Jiang P, Chang A, Xiang R, Sun P (2017) Inactivation of p38 MAPK contributes to stem cell-like properties of non-small cell lung cancer. Oncotarget 8: 26702-26717.

Guo J, Li M, Meng X, Sui J, Dou L, Tang W, Huang X, Man Y, Wang S, Li J (2014) MiR-291b-3p induces apoptosis in liver cell line NCTC1469 by reducing the level of RNA-binding protein HuR. Cell Physiol Biochem 33: 810-822.

He L, Wang X, Liu K, Wu X, Yang X, Song G, Zhang B, Zhong L (2018) Integrative PDGF/PDGFR and focal adhesion pathways are downregulated in ERCC1-defective non-small cell lung cancer undergoing sodium glycididazole-sensitized cisplatin treatment. Gene 691: 70-76.

Horn L, Infante JR, Reckamp KL, Blumenschein GR, Leal TA, Waqar SN, Gitlitz BJ, Sanborn RE, Whisenant JG, Du L, Neal JW, Gockerman JP, Dukart G, Harrow K, Liang C, Gibbons JJ, Holzhausen A, Lovly CM, Wakelee HA (2018) Ensartinib (X-396) in ALK-positive non-small cell lung cancer: results from a first-in-human phase I/II, multicenter study. Clin Cancer Res 24: 2771-2779.

Howe GA, Xiao B, Zhao H, Al-Zahrani KN, Hasim MS, Villeneuve J, Sekhon HS, Goss GD, Sabourin LA, Dimitroulakos J, Addison CL (2016) Focal adhesion kinase inhibitors in combination with erlotinib demonstrate enhanced anti-tumor activity in non-small cell lung cancer. PLoS One 11: e0150567.

Hsu NY, Chen CY, Hsu CP, Lin TY, Chou MC, Chiou SH, Chow KC (2007) Prognostic significance of expression of nm23-H1 and focal adhesion kinase in non-small cell lung cancer. Oncol Rep 18: 81-85.

Ishiguro F, Murakami H, Mizuno T, Fujii M, Kondo Y, Usami N, Taniguchi T, Yokoi K, Osada H, Sekido Y (2013) Membranous expression of activated leukocyte cell adhesion molecule contributes to poor prognosis and malignant phenotypes of non-small-cell lung cancer. J Surg Res 179: 24-32.

Jassam SA, Maherally Z, Smith JR, Ashkan K, Roncaroli F, Fillmore HL, Pilkington GJ (2017) CD15s/CD62E Interaction mediates the adhesion of non-small cell lung cancer cells on brain endothelial cells: implications for cerebral metastasis. Int J Mol Sci 18: pii: E1474.

Kitano H, Chung JY, Ylaya K, Conway C, Takikita M, Fukuoka J, Doki Y, Hanaoka J, Hewitt SM (2014) Profiling of phospho-AKT, phospho-mTOR, phospho-MAPK and EGFR in non-small cell lung cancer. J Histochem Cytochem 62: 335-346.

Kuang BH, Wen XZ, Ding Y, Peng RQ, Cai PQ, Zhang MQ, Jiang F, Zhang XS, Zhang X (2013) The prognostic value of platelet endothelial cell adhesion molecule-1 in non-small-cell lung cancer patients. Med Oncol 30: 536.

Lin CH, Lin HH, Kuo CY, Kao SH (2017) Aeroallergen Der p 2 promotes motility of human non-small cell lung cancer cells via toll-like receptor-mediated up-regulation of urokinase-type plasminogen activator and integrin/focal adhesion kinase signaling. Oncotarget 8: 11316-11328.

Livak KJ, Schmittgen TD (2001) Analysis of relative gene expression data using real-time quantitative PCR and the 2(-delta delta C(T)) method. Methods 25: 402-408.

Min HY, Jung Y, Park KH, Oh WK, Lee HY (2018) Erybraedin A is a potential Src inhibitor that blocks the adhesion and viability of non-small-cell lung cancer cells. Biochem Biophys Res Commun 502: 145-151.

Ntantie E, Allen MJ, Fletcher J, Nkembo AT, Lamango NS, Ikpatt OF (2018) Suppression of focal adhesion formation may account for the suppression of cell migration, invasion and growth of non-small cell lung cancer cells following treatment with polyisoprenylated cysteinyl amide inhibitors. Oncotarget 9: 25781-25795.

Ruder D, Papadimitrakopoulou V, Shien K, Behrens C, Kalhor N, Chen H, Shen L, Lee JJ, Hong WK, Tang X, Girard L, Minna JD, Diao L, Wang J, Mino B, Villalobos P, Rodriguez-Canales J, Hanson NE, Sun J, Miller V, Greenbowe J, Frampton G, Herbst RS, Baladandayuthapani V, Wistuba II, Izzo JG (2018) Concomitant targeting of the mTOR/MAPK pathways: novel therapeutic strategy in subsets of RICTOR/KRAS-altered non-small cell lung cancer. Oncotarget 9: 33995-34008.

Singhi EK, Horn L (2018) Background and rationale of the eXalt3 trial investigating X-396 in the treatment of ALK+ non-small-cell lung cancer. Future Oncol 14: 1781-1787.

Su CY, Li YS, Han Y, Zhou SJ, Liu ZD (2014) Correlation between expression of cell adhesion molecules CD(4)(4) v6 and E-cadherin and lymphatic metastasis in non-small cell lung cancer. Asian Pac J Cancer Prev 15: 2221-2224.

Tachezy M, Zander H, Wolters-Eisfeld G, Muller J, Wicklein D, Gebauer F, Izbicki JR, Bockhorn M (2014) Activated leukocyte cell adhesion molecule (CD166): an "inert" cancer stem cell marker for non-small cell lung cancer? Stem Cells 32: 1429-1436.

Wang HY, Hsu MK, Wang KH, Tseng CP, Chen FC, Hsu JT (2016) Non-small-cell lung cancer cells combat epidermal growth factor receptor tyrosine kinase inhibition through immediate adhesion-related responses. Onco Targets Ther 9: 2961-2973.

Webber PJ, Park C, Qui M, Ramalingam SS, Khuri FR, Fu H, Du Y (2015) Combination of heat shock protein 90 and focal adhesion kinase inhibitors synergistically inhibits the growth of non-small cell lung cancer cells. Oncoscience 2: 765-776.

Zhang B, Zhang H, Shen G (2016) Metastasis-associated protein 2 (MTA2) promotes the metastasis of non-small-cell lung cancer through the inhibition of the cell adhesion molecule Ep-CAM and E-cadherin. Jpn J Clin Oncol 46: 393.

Zhang C, Zhu H, Yang X, Lou J, Zhu D, Lu W, He Q, Yang B (2010) P53 and p38 MAPK pathways are involved in MONCPT-induced cell cycle G2/M arrest in human non-small cell lung cancer A549. J Cancer Res Clin Oncol 136: 437-445.

Zheng G, Shen Z, Chen H, Liu J, Jiang K, Fan L, Jia L, Shao J (2017) Metapristone suppresses non-small cell lung cancer proliferation and metastasis via modulating RAS/RAF/MEK/MAPK signaling pathway. Biomed Pharmacother 90: 437-445.

Zhou B, Wang GZ, Wen ZS, Zhou YC, Huang YC, Chen Y, Zhou GB (2018) Somatic mutations and splicing variants of focal adhesion kinase in non-small cell lung cancer. J Natl Cancer Inst 110: doi: 10.1093/jnci/djx157.